pISSN 1229-3008 eISSN 2287-6251
Progress in Superconductivity and Cryogenics
Vol.21, No.1, (2019), pp.31~35 https://doi.org/10.9714/psac.2019.21.1.031

Contact resistance increment of no-insulation REBCO magnet during a quench

Chaemin Im, Mincheol Cho, Jeseok Bang, Jaemin Kim, and Seungyong Hahn*

Department of Electrical and Computer Engineering, Seoul National University, Seoul, 08826, South Korea

(Received 15 February 2019; revised or reviewed 27 March 2019; accepted 28 March 2019)

Abstract

The lumped-parameter circuit model for a no- insulation (NI) high temperature superconductor (HTS) magnet has been well understood after many experimental and analytic studies over a decade. It successfully explains the non-linear charging behaviors of NI magnets. Yet, recently, multiple groups reported that the post-quench electromechanical behaviors of an NI HTS magnet may not be well explained by the lumped circuit model. The characteristic resistance of an NI magnet is one of the key parameters to characterize the so-called "NI behaviors" of an NI magnet and recently a few groups reported a potential that the characteristic resistance of an NI magnet may substantially vary during a quench. This paper deals with this issue, the increment of contact resistance of the no-insulation (NI) REBCO magnet during a quench and its impact on the post-quench behaviors. A 7 T 78 mm NI REBCO magnet that was previously built by the MIT Francis Bitter Magnet Laboratory was chosen for our simulation to investigate the increment of contact resistance to better duplicate the post-quench coil voltages in the simulation. The simulation results showed that using the contact resistance value measured in the liquid nitrogen test, the magnitude of the current through the coil must be much greater than the critical current. This indicates that the value of the contact resistance should increase sharply after the quench occurs, depending on the lumped circuit model.

Keywords: contact resistance, lumped circuit model, no - insulation, quench

1. INTRODUCTION

Since no-insulation(NI) characteristics were observed in 2011 [1], various analyzing methods have been developed and used to date [1–13]. These methods can be classified into two types, a method with the lumped-parameter circuit and the distributed network circuit. The lumped-parameter circuit models each double pancake (DP) into the self-inductance *L* (or mutual inductance *M*), the super-conducting variable resistor R_{sc} in series, and the resistor in parallel that indicates V-I characteristics between turn-to-turn called 'characteristic resistance', R_c, as shown in Fig. 1. The current passing through the superconducting resistor and the characteristic resistance are referred to as the azimuthal current I_θ and the radial current I_r, respectively. From the lumped-parameter circuit, various types of distributed network model have been developed. Yanagisawa et al. subdivided the entire pancake coil into multiple nodes comprising with elements [2], Wang et al. converted the whole NI coil into an equivalent circuit grid (ECG) [3], Wang et al. subdivided every turn into multiple segments and developed the partial element equivalent circuit (PEEC) model [4], and Markiewicz et al. modeled the whole coil to series of turn-distributed circuits [5].

Due to its simplicity, the computation time of the lumped-parameter circuit is much shorter than the distributed network circuit. Also, its accuracy has verified in current charging and discharging simulation compared with the experiment below critical current [6]. However, since the entire magnet or each DP is modeled as a single circuit, there are some limitations in analyzing internal local electromagnetic phenomena using the lumped-parameter circuit [2]. These limitations are apparent when quench occurs, as numerous physical phenomena, such as overcurrent, overstress, and heat dissipation, occur simultaneously within a magnet or DP due to normal-zone transition during a quench [14, 15].

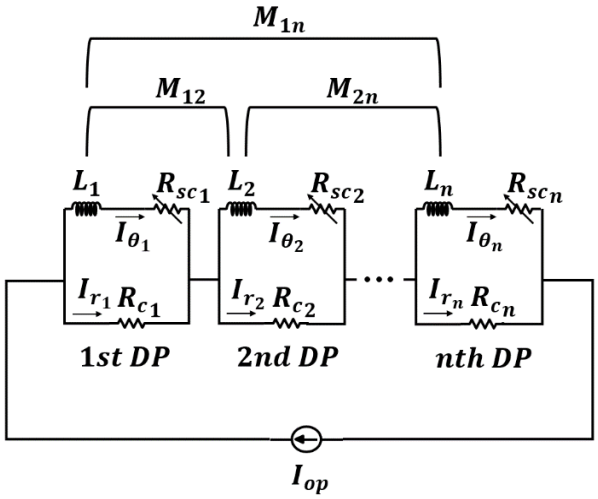

Fig. 1. A lumped-parameter circuit model consisting of n-DPs [18].

* Corresponding author: hahnsy@snu.ac.kr

In this paper, a quench analysis using the lumped - parameter circuit was performed. The configuration and experimental results of a 7 T 78 mm NI REBCO coil produced by the MIT Fancis Bitter Magnet Laboratory were used for analyzing simulation [16]. The azimuthal current and the radial current were simulated based on the experimentally measured DP voltage and the total operating current measured by the shunt resistor. The characteristic resistance at 77 K was also used in simulation. The value of the characteristic resistance was set to increase from half of the measured value to the measured value with reference to the results of Lu et al [17]. However, each simulated currents was much larger than the critical current level [18–24]. From this simulation, the results suggest that a sharp increase in contact resistance will occur during a quench.

2. 7 T 78 MM MAGNET CONFIGURATION AND PARAMETERS

The configuration of the 7 T 78 mm magnet is presented in Fig. 2. The magnet consists of 13 DPs numbered from top to bottom and is modeled as a series of 13 lumped-parameter circuits. Parameters of each DP are solved by Kirchhoff's voltage law and Kirchhoff's current law.

2.1. Parameters of the REBCO conductor

The parameters of REBCO conductor are shown in Table I. The tapes were manufactured from SuNAM and have multiple average widths from 4.1 mm to 8.1 mm. The average thickness of the tape was 85 μm and had a residual resistivity ratio(RRR) 50 copper stabilizer with an average 10 μm thickness at each side.

TABLE I
REBCO CONDUCTOR PARAMETERS [25].

Parameters	Units	Value
Average Width	[mm]	4.1;5.1;6.1;7.1;8.1
Average Thickness	[μm]	85
Copper Stabilizer Thickness	[μm]	10 per side

Maunfactured by SuNAM Co.

2.2. Parameters of the Magnet

The parameters of 7 T 78 mm magnet are shown in Table II. Since the magnet was wound in multi-width (MW) technique [26, 27], DPs have the same width are called a module. Five modules constitute the magnet, and the thickness of each module is in ascending order from middle to edge, from 4.1 mm to 8.1 mm. The inner diameter and the outer diameter of the magnet are 78.0 mm and 101.8 mm each, and the average number of turns per DP is 280. The value of the characteristic resistance was 1.4 mΩ in 77 K. From the characteristic resistance, the average contact resistance can be derived which is presented in Eq. (1) [28]. In this equation, N is the total number of turns, r_i is the radius of i^{th} turn and w_k is the width of the k^{th} module. From this equation, the contact resistance value was 5.6 μΩ · cm^2.

$$R_c = \sum_{i=1}^{N} \frac{R_{ct}}{2\pi r_i w_k} \tag{1}$$

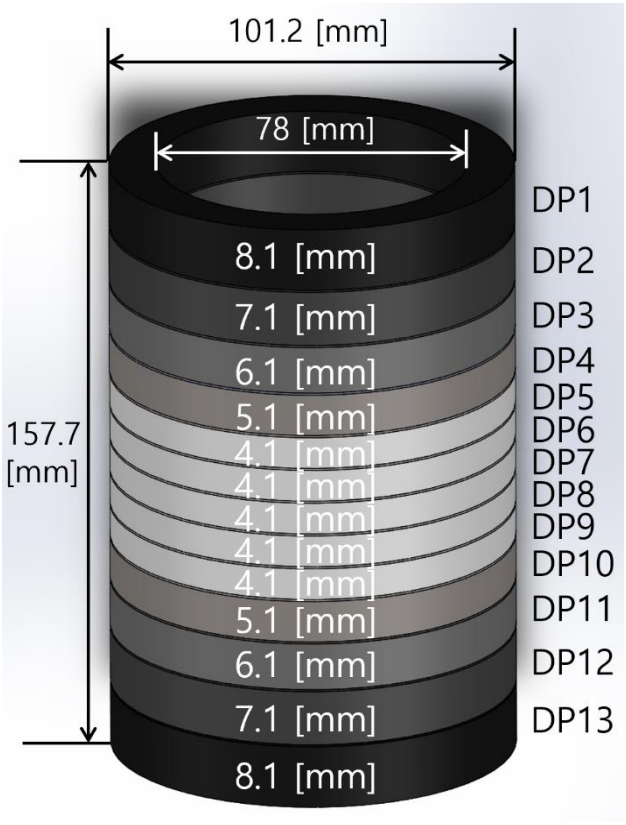

Fig. 2. Schematic of 7 T 78 mm magnet configuration [16].

TABLE II
7T 78MM MAGNET PARAMETERS [16].

Parameters	Units	MD.1	MD.2	MD.3	MD.4	MD.5
Magnet Configuration						
Average Width	[mm]	4.1	5.1	6.1	7.1	8.1
Number of DP	[mm]	5	2	2	2	2
Coil I.D.; O.D.	[mm]	78.0;101.8				
Turns per Pancake		140				
Winding tension	[MPa]	56				
Operation						
Operating Current, I_{op}	[A]	312				
Characteristic Resistance, R_c	[mΩ]	1.4				
Contact Resistance, R_{ct}	[$\mu\Omega$·cm^2]	5.6				
Total Inductance, L	[H]	0.521				

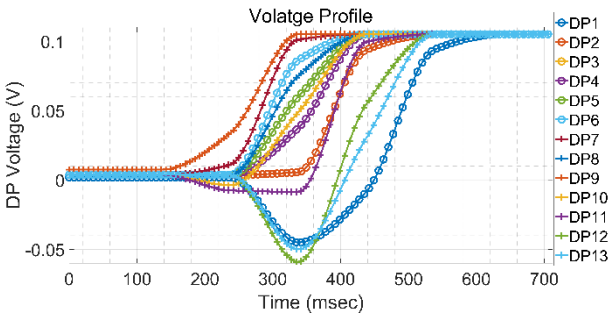

Fig. 3. Voltage profile of the 7 T 78 mm magnet quench experiment interpolated with the Hermite method.

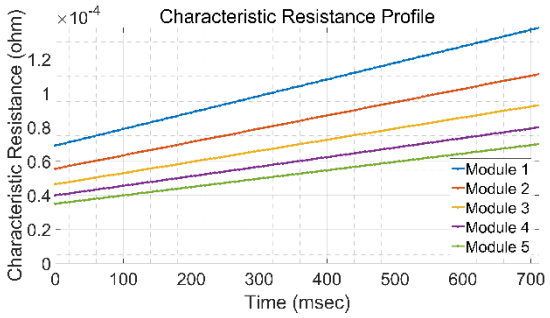

Fig. 4. Characteristic resistance of each module.

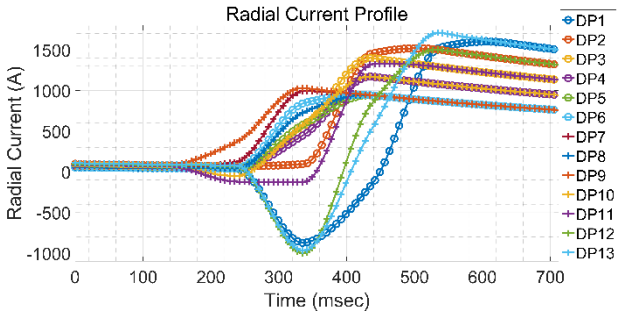

Fig. 6. Simulated radial current profile with characteristic resistance measured at 77 K.

3. SIMULATION RESULTS & DISCUSSION

3.1. Key Equations: KVL and KCL

Prior to the simulation results, the equations used in the simulation is presented. In a lumped-parameter circuit shown in Fig. 1, KVL and KCL in Eq. (2) and Eq. (3) are applied to each circuit.

$$V_n = I_{\theta_n} R_{sc_n} + \sum_{i=1}^{n} \sum_{j=1}^{n} M_{ij} \frac{dI_\theta}{dt} = I_{r_n} R_{c_n} \quad (2)$$

$$I_{op} = I_{\theta_n} + I_{r_n} \quad (3)$$

In these equations, $V_n, I_{\theta_n}, R_{sc_n}, I_{r_n}$ and R_{c_n} are voltage, azimuthal current, superconductor resistance, radial current and characteristic resistance of n^{th} DP, respectively. M_{ij} represents the mutual inductance of i^{th} and j^{th} DP, where I_{op} represents the operating current measured by shunt resistor.

3.2. Coil Voltage: Interpolated by Hermite method

Since the results of the experiment included only 9 data sets per DP, they were interpolated by the Hermite method [29]. Fig. 3 shows the interpolated voltage profile. The initial rising of the voltage indicates the quench initiation at DP 9. The voltages over 0.1 V were not measured accurately due to measurement limitations. In other words, the actual voltage would have exceeded the measured voltage level.

3.3. Azimuthal & Radial Current Simulation: by Adopting Measured Characteristic Resistance Value

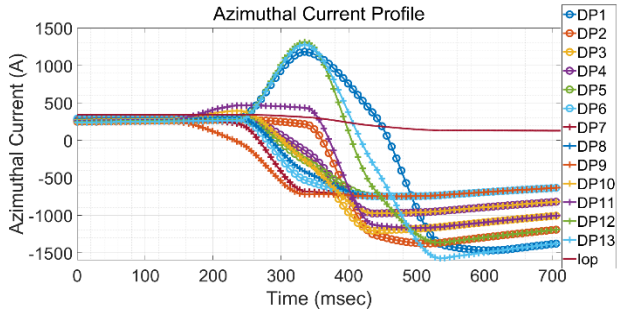

Fig. 5. Simulated azimuthal current & operating current profile with characteristic resistance measured at 77 K.

Fig. 4 shows the characteristic resistance profile of each module used in the simulation. From energy conservation equation, the final temperature after quench is 76.9 K [18] and according to J. Lu, the value of the contact resistance increases from 4.2 K to 77 K about 2 times [17]. Thus, in this simulation, half of the measured value in 77 K was assumed to the initial characteristic resistance and contact resistance and both of them increased linearly. The initial contact resistance value of all modules was 2.8 $\mu\Omega \cdot cm^2$ and it increased to the final value 5.6 $\mu\Omega \cdot cm^2$.

Fig. 5 and Fig. 6 show the simulated azimuthal current, operating current and radial current calculated from the Eq. (2) and Eq. (3). The operating current decreased from 343 A to 128 A. The peak value of the azimuthal current was about 1310 A, where the negative peak value of the radial current was about -1000 A, both of which flowed in DP12. The values of critical current (I_c) of each DP at 4.2 K are about 300-500 A level, well below the simulated azimuthal /radial current values [18]. This can be interpreted in the value of the contact resistance need to be increased.

3.4. Azimuthal Current Simulation: by Adopting Increased Characteristic Resistance Value

It is not clear how the azimuthal current should actually flow. However, applying the assumption that at least the azimuthal current should not decrease to a negative value, in other words, the radial current should not exceed the operating current, the result indicates that the ramping rate of the contact resistance should increase into at least 14-29 times, which makes the value of the characteristic resistance of every coil to about 0.1 mΩ at the end of the quench. Fig. 7 shows azimuthal current profile when the

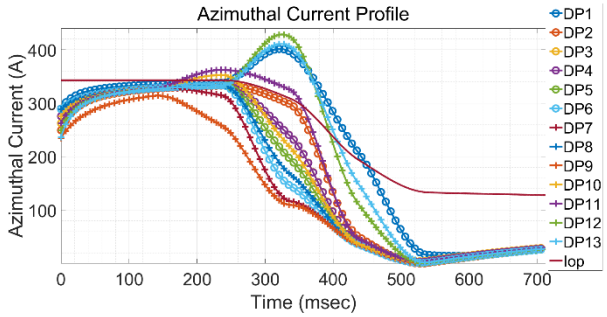

Fig. 7. Simulated azimuthal current & operating current profile with increased characteristic resistance ramps to 0.1 mΩ.

value of characteristic resistance of all DPs are ramped from half of 77 K measured value to 0.1 mΩ.

4. CONCLUSION

The 7 T 78mm magnet experimental result was analyzed with the lumped-parameter circuit. Applying KVL and KCL to each coil, the azimuthal current and the radial current value were simulated from measured voltage, operating current and ramping characteristic resistance from half to the 77 K value. However, the peak values of both currents were far above the estimated critical current value. Therefore, the drastic increment of contact resistance during a quench was suggested to explain this result. However, since the lumped-parameter circuit has a limitation of analyzing internal phenomenon and the measured voltage of the 7 T 78 mm magnet quench experiment was saturated at 0.1 V, a study using a distributed network circuit with data whose voltage value is not saturated should be followed.

ACKNOWLEDGMENT

This work was supported by Samsung Research Funding & Incubation Center of Samsung Electronics under Project Number SRFC-IT1801-09.

REFERENCES

[1] S. Hahn, D. K. Park, J. Bascuñán, and Y. Iwasa, "HTS pancake coils without turn-to-turn insulation," *IEEE Transactions on Applied Superconductivity*, vol. 21, no. 3, pp. 1592–1595, 2011.

[2] Y. Yanagisawa, K. Sato, K. Yanagisawa, H. Nakagome, X. Jin, M. Takahashi, and H. Maeda, "Basic mechanism of self-healing from thermal runaway for uninsulated REBCO pancake coils," *Physica C*, vol. 499, pp. 40–44, 2014.

[3] Y. Wang, H. Song, D. Xu, Z. Li, Z. Jin, and Z. Hong, "An equivalent circuit grid model for no-insulation HTS pancake coils," *Superconductor Science and Technology*, vol. 28, no. 4, p. 045017, 2015.

[4] T. Wang, S. Noguchi, X. Wang, I. Arakawa, K. Minami, K. Monma, A. Ishiyama, S. Hahn, and Y. Iwasa, "Analyses of transient behaviors of no-insulation REBCO pancake coils during sudden discharging and overcurrent," *IEEE Transactions on Applied Superconductivity*, vol. 25, no. 3, p. 4603409, 2015.

[5] W. D. Markiewicz, J. J. Jaroszynski, D. V. Abraimov, R. E. Joyner, and A. Khan, "Quench analysis of pancake wound REBCO coils with low resistance between turns," *Superconductor Science and Technology*, vol. 29, no. 2, p. 025001, 2015.

[6] J. Kim, S. Yoon, K. Cheon, K. H. Shin, S. Hahn, D. L. Kim, S. Lee, H. Lee, and S.-H. Moon, "Effect of resistive metal cladding of HTS tape on the characteristic of no-insulation coil," *IEEE Transactions on Applied Superconductivity*, vol. 26, no. 4, p. 4601906, 2016.

[7] D. G. Yang, S. Hahn, Y. Kim, K. L. Kim, J.-B. Song, J. Bascuñán, H. Lee, and Y. Iwasa, "Characteristic resistance of no-insulation and partial-insulation coils with nonuniform current distribution," *IEEE Transactions on Applied Superconductivity*, vol. 24, no. 3, p. 7700405, 2014.

[8] Y. J. Hwang, J. Y. Jang, S. Song, J. M. Kim, and S. Lee, "Feasibility study of the impregnation of a no-insulation HTS coil using an electrically conductive epoxy," *IEEE Transactions on Applied Superconductivity*, vol. 27, no. 4, p. 4603405, 2017.

[9] J. Y. Jang, S. Yoon, S. Hahn, Y. J. Hwang, J. Kim, K. H. Shin, K. Cheon, K. Kim, S. In, Y.-J. Hong et al., "Design, construction and 13 K conduction-cooled operation of a 3 T 100 mm stainless steel cladding all- REBCO magnet," *Superconductor Science and Technology*, vol. 30, no. 10, p. 105012, 2017.

[10] Y. Li, D. Hu, J. Zhang, W. Wu, Z. Li, K. Ryu, Z. Hong, and Z. Jin, "Feasibility study of the impregnation of a no-insulation hts coil using solder," *IEEE Transactions on Applied Superconductivity*, vol. 28, no. 1, p. 5200505, 2018.

[11] Y. Wang, W. K. Chan, and J. Schwartz, "Self-protection mechanisms in no-insulation (RE) Ba2 Cu3 Ox high temperature superconductor pancake coils," *Superconductor Science and Technology*, vol. 29, no. 4, p. 045007, 2016.

[12] H. Song and Y. Wang, "Simulations of nonuniform behaviors of multiple No-insulation (RE) Ba2 Cu3 O7-x HTS pancake coils during charging and discharging," *IEEE Transactions on Applied Superconductivity*, vol. 26, no. 4, p. 4700105, 2016.

[13] S. Noguchi, K. Kim, and S. Hahn, "Simulation on electrical field generation by hall effect in no-insulation REBCO pancake coils," *IEEE Transactions on Applied Superconductivity*, vol. 28, no. 3, p. 4901805, 2018.

[14] Y. G. Park, H. C. Jo, J. Lee, H. M. Kim, Y. Do Chung, Y. Chu, K. Y. Yoon, T. K. Ko, and Y. S. Yoon, "Test and analysis of electromagnetic and mechanical properties of hts coil during quench state," *IEEE Transactions on Applied Superconductivity*, vol. 26, no. 3, p. 4602104, 2016.

[15] A. Ikeda, T. Oki, T. Wang, A. Ishiyama, K. Monma, S. Noguchi, T. Watanabe, and S. Nagaya, "Transient behaviors of no-insulation REBCO pancake coil during local normal-state transition," *IEEE Transactions on Applied Superconductivity*, vol. 26, no. 4, p. 4600204, 2016.

[16] J.-B. Song, S. Hahn, T. Le´crevisse, J. Voccio, J. Bascun˜a´n, and Y. Iwasa, "Over-current quench test and self-protecting behavior of a 7 T/78 mm multi-width no-insulation REBCO magnet at 4.2 K," *Superconductor Science and Technology*, vol. 28, no. 11, p. 114001, 2015.

[17] J. Lu, J. Levitan, D. McRae, and R. P. Walsh, "Contact resistance between two REBCO tapes: the effects of cyclic loading and surface coating," *Superconductor Science and Technology*, vol. 31, no. 8, p. 085006, 2018.

[18] K. R. Bhattarai, K. Kim, S. Kim, S. Lee, and S. Hahn, "Quench analysis of a multiwidth no-insulation 7-T 78-mm REBCO magnet," *IEEE Transactions on Applied Superconductivity*, vol. 27, no. 4, p. 4603505, 2017.

[19] J. Y. Coulter, J. Hanisch, J. O. Willis, L. Civale, and W. K. Pierce, "Position and magnetic field angle dependent for long-length coated conductors," *IEEE Transactions on Applied Superconductivity*, vol. 17, no. 2, pp. 3394–3397, 2007.

[20] J. Y. Coulter, T. G. Holesinger, J. A. Kennison, J. O. Willis, and M. W. Rupich, "Nondestructive investigation of position dependent variations in multi-meter coated conductors," *IEEE Transactions on Applied Superconductivity*, vol. 19, no. 3, pp. 3609–3613, 2009.

[21] V. Selvamanickam, Y. Yao, Y. Chen, T. Shi, Y. Liu, N. Khatri, J. Liu, C. Lei, E. Galstyan, and G. Majkic, "The low-temperature, high-magnetic-field critical current characteristics of zr-added (gd, y) ba2cu3ox superconducting tapes," *Superconductor Science and Technology*, vol. 25, no. 12, p. 125013, 2012.

[22] S. Fujita, H. Satoh, M. Daibo, Y. Iijima, M. Itoh, H. Oguro, S. Awaji, and K. Watanabe, "Characteristics of rebco coated conductors for 25t cryogen-free superconducting magnet," *IEEE Transactions on Applied Superconductivity*, vol. 25, no. 3, p. 8400304, 2015.

[23] S. Hahn, K. Radcliff, K. Kim, S. Kim, X. Hu, K. Kim, D. V. Abraimov, and J. Jaroszynski, "'Defect-irrelevant' behavior of a no-insulation pancake coil wound with REBCO tapes containing multiple defects," *Superconductor Science and Technology*, vol. 29, no. 10, p. 105017, 2016.

[24] L. Rossi, X. Hu, F. Kametani, D. Abraimov, A. Polyanskii, J. Jaroszyn- ski, and D. Larbalestier, "Sample and length-dependent variability of 77 and 4.2 k properties in nominally identical RE123 coated conductors," *Superconductor Science and Technology*, vol. 29, no. 5, p. 054006, 2016.

[25] S. Hahn, J. Song, Y. Kim, T. Le´crevisse, Y. Chu, J. Voccio, J. Bascun˜a´n, and Y. Iwasa, "Construction and test of 7-T/68-mm cold-bore multiwidth no-insulation GdBCO magnet," *IEEE Transactions on Applied Superconductivity*, vol. 25, no. 3, p. 4600405, 2015.

[26] S. Hahn, Y. Kim, D. Keun Park, K. Kim, J. P. Voccio, J. Bascuñán, and Y. Iwasa, "No-insulation multi-width winding technique for high

temperature superconducting magnet," *Applied physics letters*, vol. 103, no. 17, p. 173511, 2013.

[27] S. Yoon, J. Kim, K. Cheon, H. Lee, S. Hahn, and S.-H. Moon, "26 T 35 mm all-GdBa2Cu3O7–x multi-width no-insulation superconducting magnet," *Superconductor Science and Technology*, vol. 29, no. 4, p. 04LT04, 2016.

[28] X. Wang, S. Hahn, Y. Kim, J. Bascunan, J. Voccio, H. Lee, and Y. Iwasa, "Turn-to-turn contact characteristics for an equivalent circuit model of no-insulation ReBCO pancake coil," *Superconductor Science and Technology*, vol. 26, no. 3, p. 035012, 2013.

[29] K. Ho¨llig and J. Koch, "Geometric hermite interpolation with maximal order and smoothness," *Computer Aided Geometric Design*, vol. 13, no. 8, pp. 681–695, 1996.